Electronic Supplementary Material (ESI) for Physical Chemistry Chemical Physics.

Supporting Information

A Mechanistic Investigation of Morphology Evolution in P3HT/PCBM Films Induced by Liquid Crystalline Molecules under External Electric Field

Weihua Zhou[1,3], Jiangman Shi[1], Lingjian Lv[1], Lie Chen[1,2], Yiwang Chen[*1,2]

[1]Institute of Polymers/Department of Chemistry, Nanchang University, 999 Xuefu Avenue, Nanchang 330031, China; [2]Jiangxi Provincial Key Laboratory of New Energy Chemistry, Nanchang University, 999 Xuefu Avenue, Nanchang 330031, China; [3]State Key Laboratory of Luminescent Materials and Devices, South China University of Technology, Guangzhou 510640, China

[*] Corresponding author. Tel.: +86 791 83969562; fax: +86 791 83969561. *E-mail address*: ywchen@ncu.edu.cn (Y. Chen).

Experimental

Materials

Regioregular P3HT ((M_w = 48300 g·mol^{-1}, head-to-tail regioregularity > 90%) and $PC_{61}BM$ (99.5% purity) used in this study were purchased from Rieke Metals, Inc. and Nano-C, respectively. Poly(3,4-ethylenedioxythiophene):poly(styrenesulfonate) (PEDOT:PSS) (Clevios, Heraeus PVP Al 4083) was obtained from Bayer Inc, whereas indium tin oxide (ITO) glass was purchased from Delta Technologies Limited. 4-cyano-4'-pentylterphenyl (5CT) was supplied by Energy Chemical Co. Dicholorobenzene (DCB) was purchased from Aldrich. All the reagents were used directly as received without further purification.

PSC device fabrication

The polymer solar cells were fabricated on ITO coated glass substrates. The ITO glass was cleaned through sequential ultrasonic treatment in acetone, detergent, deionized water, and isopropanol, and then treated in an ultraviolet-ozone chamber for 10 min. Then, a thin layer of PEDOT:PSS was spin-coated onto the ITO electrode at 4000 rpm for 60 s to give a film with the thickness of about 40 nm. The substrates were baked on a hot plate at 140 ºC for 20 min, to ensure the thorough evaporation of residual water. Subsequently, the ternary blend solution containing different weight fraction of 5CT was spin-coated on top of PEDOT:PSS layer at 800 rpm for 30 s. The electric field assisted treatment was then performed by applying various magnitudes of voltage during the solvent drying process for 30 min in air. The structure of the electric field equipment is illustrated in **Figure 1a**. For the specimens without electric field assisted treatment, they were also slowly dried in the same equipment after the solvent evaporation in air. Afterwards, a cathode consisting of a LiF (1 nm) layer and a subsequent Al (100 nm) layer was deposited by thermal evaporation under a vacuum of 10^{-7} Torr. Devices with the configuration of ITO/PEDOT:PSS/P3HT:PCBM:5CT/LiF/Al were encapsulated with a glass cap to protect them from air. The active area of all devices was defined as 4 mm^2 by a

shadow mask. For the devices with the configuration of ITO/PEDOT:PSS/P3HT:PCBM:5CT/MoO_3/Ag, using for the space-charge-limited-current (SCLC) hole mobility measurement,[1-3] the fabrication process is similar to that of solar cell device. Similarly, an electrode consisting of a MoO_3 (10 nm) layer and a subsequent Ag (100 nm) layer was deposited by thermal evaporation under a vacuum of 10^{-7} Torr. For the electron-only devices using a diode configuration of ITO/ZnO/P3HT:PCBM:5CT/LiF/Al, the fabrication process was similar to the devices as described above.

Measurements

The miscibility between P3HT and 5CT, and interactions between PCBM and 5CT were characterized by the differential scanning calorimetry (DSC) analysis. The P3HT/5CT, PCBM/5CT and P3HT/PCBM/5CT blends at different weight fraction of 5CT were prepared by the solution blending method. The specimens of about 3 mg were heated to 300 ºC at a rate of 10 ºC/min. After 3 min, the specimens were cooled to room temperature at a rate of 10 ºC/min. The liquid crystalline transition temperature of LCs, as well as the melting temperature (T_m) of P3HT or PCBM was analyzed based on the DSC heating curves. The crystallization peak temperature (T_c) of P3HT or PCBM was analyzed based on the DSC cooling curves. The morphology of the films with or without electric field assisted treatment was observed by the polarized optical microscopy (POM) (NIKON E600 POL) equipped with a camera. The UV-visible absorption spectra of P3HT/5CT and P3HT/PCBM/5CT films were measured using a Perkin-Elmer Lambda 750 UV/VIS spectrometer. The morphology of the films was conducted by employing transmission electron microscopy (TEM) (JEM-2010 HR) with an accelerating voltage of 200 kV. The topography observation of P3HT/PCBM/5CT films was performed by atomic force microscopy (AFM). The photoluminescence properties were examined at the excitation wavelength of 480 nm on an LS-55 (Perkin-Elmer), for which the specimens were prepared by drop-casting. The concentration of the PCBM, P3HT, 5CT in chloroform was maintained at 10 mg/mL, and the PCBM/5CT (1:1 in weight ratio) and PCBM/P3HT (1:1 in weight

ratio) blends in chloroform was 20 mg/mL. The time-resolved photoluminescence spectra of P3HT and P3HT/5CT=1:1 were recorded by Edinburgh Instrument FLS920 at an excitation wavelength of 650 nm. Photocurrent/voltage (J/V) curves were recorded using a Keithley 2400 Source Meter under 100 mW/cm^2 simulated AM 1.5 G irradiation (Abet Solar Simulator Sun2000). The GIXRD profiles were obtained by using a Bruker D8 Discover reflector with an X-ray generation power of 40 kV tube voltage and 40 mA tube current. The measurements were obtained in a scanning interval of 2θ between 2º and 30º. To increase the GIXRD peak intensity for investigating the crystallinity and orientation that prevail throughout the film, we employed an incident angle (α = 0.21º) above the critical angle (α_c = 0.18º). GISAXS measurements were performed at the Shanghai Synchrotron Radiation Facility (SSRF) on the BL16B1 beamline using a photon energy of 10 keV with a sample to detector distance of approximately 2025 mm. The incident angle was set to 0.4º, which was above the critical angles of P3HT and PCBM and therefore the structure of the full film thickness was detected. The GISAXS signal was shielded with a rod-like beam stop, and the schematic GISAXS configuration is illustrated in **Figure 1b**. The samples using for the POM, TEM, AFM, GIXRD, GISAXS analysis were the same as those for the photovoltaic properties testing.

FIGURES

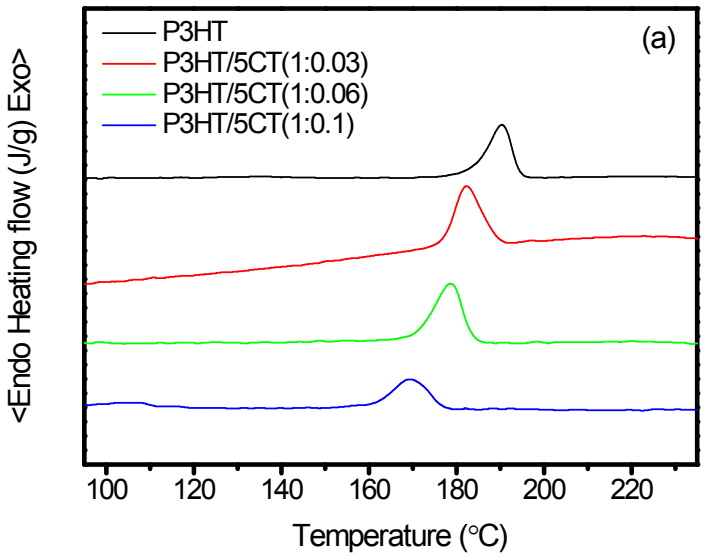
P3HT
P3HT/5CT(1:0.03)
P3HT/5CT(1:0.06)
P3HT/5CT(1:0.1)
(a)
<Endo Heating flow (J/g) Exo>
100
120
140
160
180
200
220
Temperature (°C)

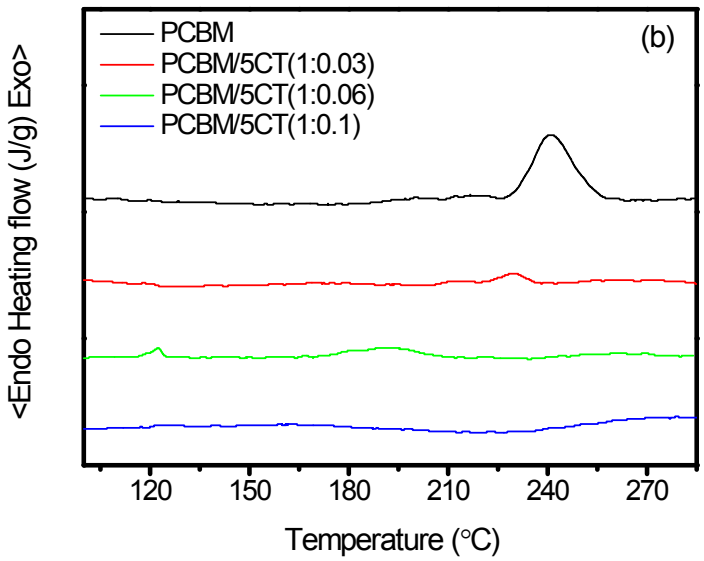
PCBM
PCBM/5CT(1:0.03)
PCBM/5CT(1:0.06)
PCBM/5CT(1:0.1)
(b)
<Endo Heating flow (J/g) Exo>
120
150
180
210
240
270
Temperature (°C)

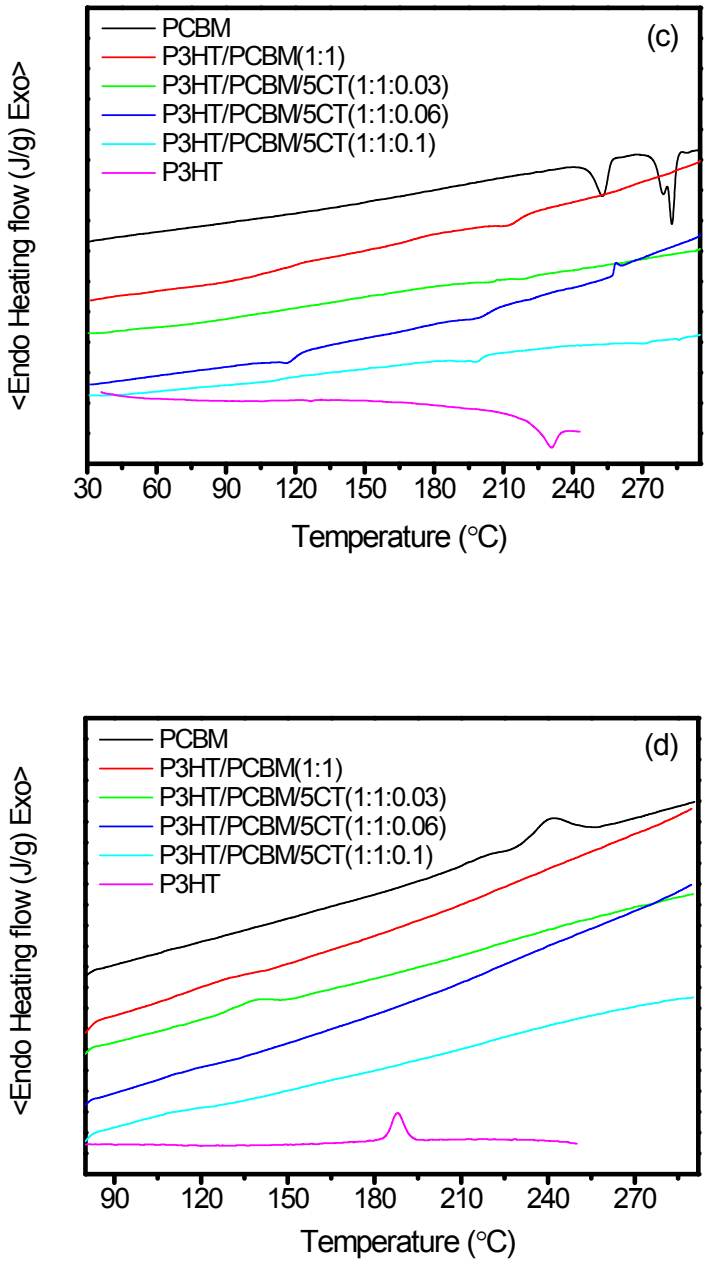

Figure S1. DSC cooling curves of (a) P3HT/5CT and (b) PCBM/5CT binary blends, and the DSC (c) heating and (d) cooling curves of P3HT/PCBM/5CT ternary blends at different weight fraction of 5CT.

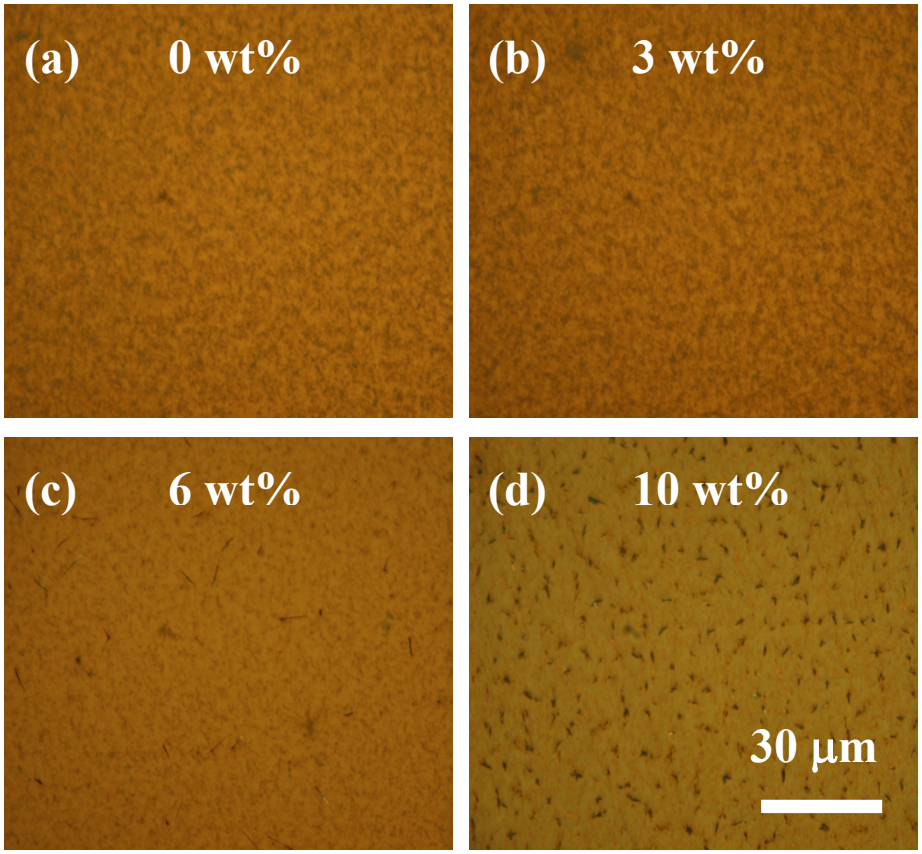

Figure S2. Dark-field POM images of P3HT/PCBM/5CT films spin-cast onto an ITO substrate containing different weight fraction of 5CT.

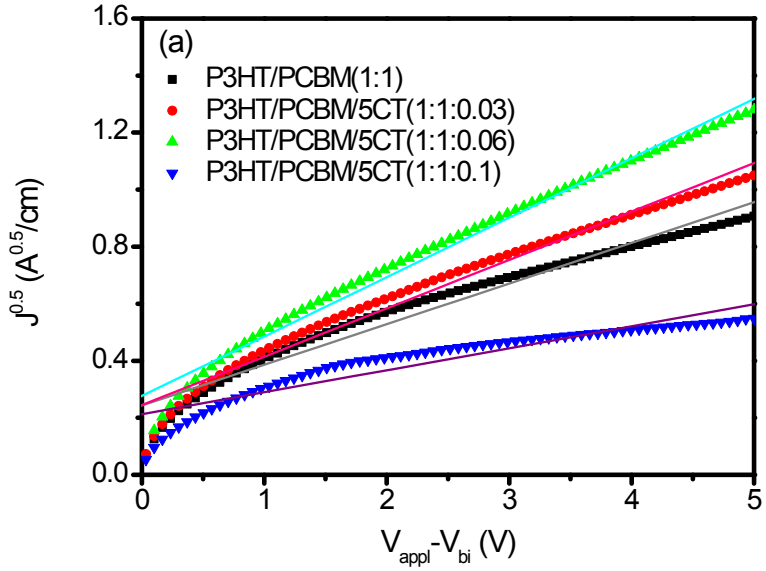
(a)
P3HT/PCBM(1:1)
P3HT/PCBM/5CT(1:1:0.03)
P3HT/PCBM/5CT(1:1:0.06)
P3HT/PCBM/5CT(1:1:0.1)
J^0.5 (A^0.5/cm)
V_appl-V_bi (V)
0.0
0.4
0.8
1.2
1.6
0
1
2
3
4
5

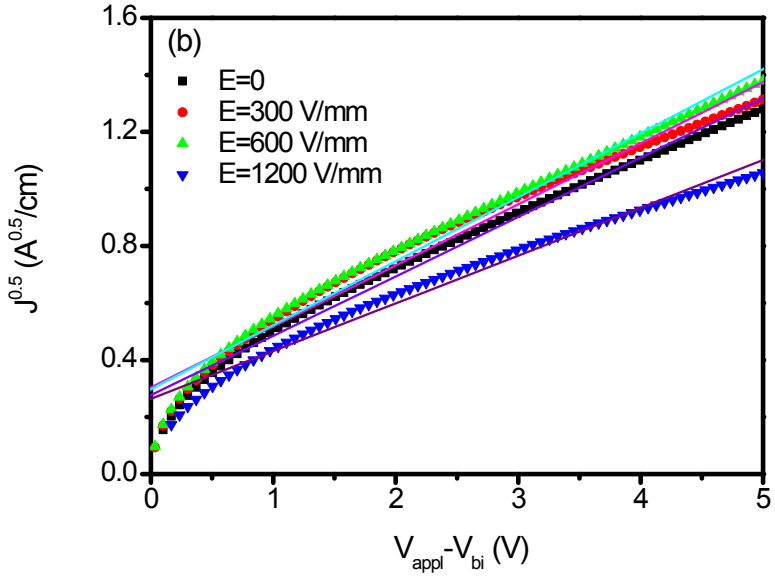
(b)
E=0
E=300 V/mm
E=600 V/mm
E=1200 V/mm
J^0.5 (A^0.5/cm)
V_appl-V_bi (V)
0.0
0.4
0.8
1.2
1.6
0
1
2
3
4
5

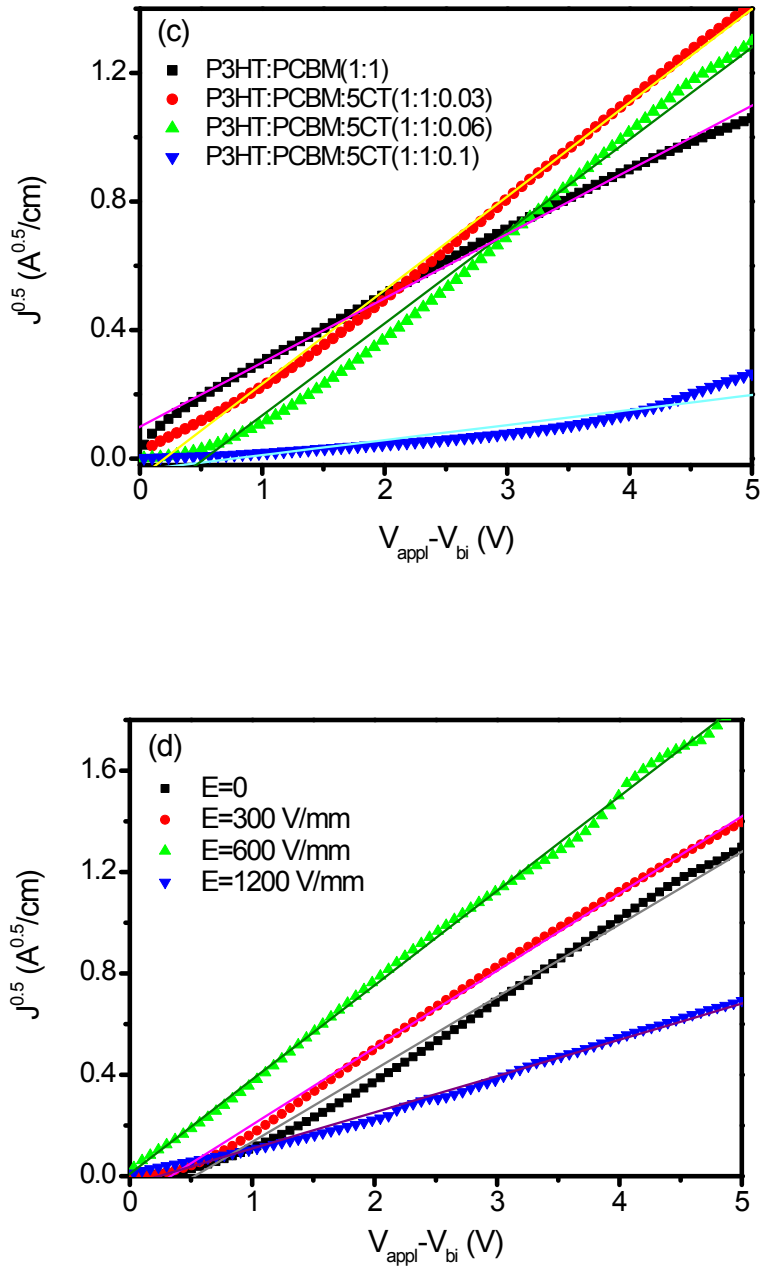

Figure S3. $J^{1/2}$-V characteristics of (a, b) hole (μ_h) mobilities and (c, d) electron (μ_e) mobilities based on P3HT/PCBM/5CT blends with different content of 5CT (a, c) and under different electric field intensities (b, d) using SCLC modeling measured at ambient temperature.

The effect of doping 5CT and electric field assisted treatment on charge transport properties was investigated. The carrier mobility was measured using the SCLC

model at low voltage which is described by following equation:

$$J=9\varepsilon_0\varepsilon_r\mu V^2/8L^3 \quad (2)$$

where ε_0 is the permittivity of free space (8.85×10^{-12} F m^{-1}), ε_r is the dielectric constant of P3HT or PCBM (assumed to 3), μ is the mobility of an electron, V is the applied voltage, and L is the film thickness.[1-3] The thickness of the BHJ blend for SCLC measurement was about 120 nm. As shown in **Figure S3** and **Table 1,** the hole mobility increased from 1.17×10^{-4} to 2.51×10^{-4} $cm^2/V\cdot s$, and the electron mobility increased from 2.39×10^{-4} to 4.63×10^{-4} $cm^2/V\cdot s$ as the 5CT weight fraction increasing to 6 wt%. However, further increase of 5CT weight fraction leads to a reduction in both of hole and electron mobilities. It is revealed that an appropriate amount of 5CT (6 wt%) in the P3HT/PCBM blend facilitated the improvement of the carrier mobility. In addition, the hole and electron mobilities are also dependent on the intensity of electric field. As the specimen containing 6 wt% 5CT is concerned, the hole mobility and electron mobility reaches to the highest value of 2.91×10^{-4} and 7.61×10^{-4} $cm^2/V\cdot s$ at the electric field intensity of 600 V/mm. The improvement of device performance is mainly due to the corresponding increase of carrier mobilities, which is actually determined by the morphology of the active layer.

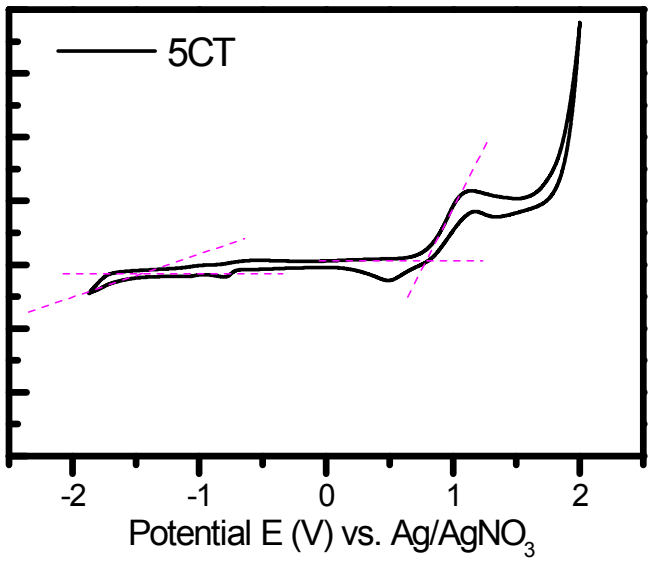

Figure S4. The cyclic voltammetry curves for 5CT molecules.

Cyclic voltammograms (CV) were performed in a three-electrode cell using platinum electrodes at a scan rate of 50 mVs^{-1} and a Ag/Ag^{+} (0.1 M of $AgNO_3$ in acetonitrile) reference electrode in an anhydrous and nitrogen-saturated solution of 0.1 M tetrabutylammonium tetrafluoroborate (Bu_4NBF_4) in acetonitrile. Under these conditions, the onset oxidation potential ($E_{1/2\ ox}$) of ferrocene was -0.02 V versus Ag/Ag^{+}. The HOMO energy level of 5CT was determined from the oxidation onset of the second scan from CV data. It is assumed that the redox potential of $FcFc^{+}$ has an absolute energy level of -4.80 eV to vacuum. The energy of HOMO and LUMO levels were calculated according to the Equation 1 and 2, and the electrochemically determined band gaps were deduced from the difference between onset potentials from oxidation and reduction of copolymers as depicted in Equation 3.

$$E_{HOMO} = -(E_{onset}^{ox} + 4.82)(eV) \quad (1)$$

$$E_{LUMO} = -(E_{onset}^{red} + 4.82)(eV) \quad (2)$$

$$E_{gap}^{EC} = (E_{onset}^{ox} - E_{onset}^{red})(eV) \quad (3)$$

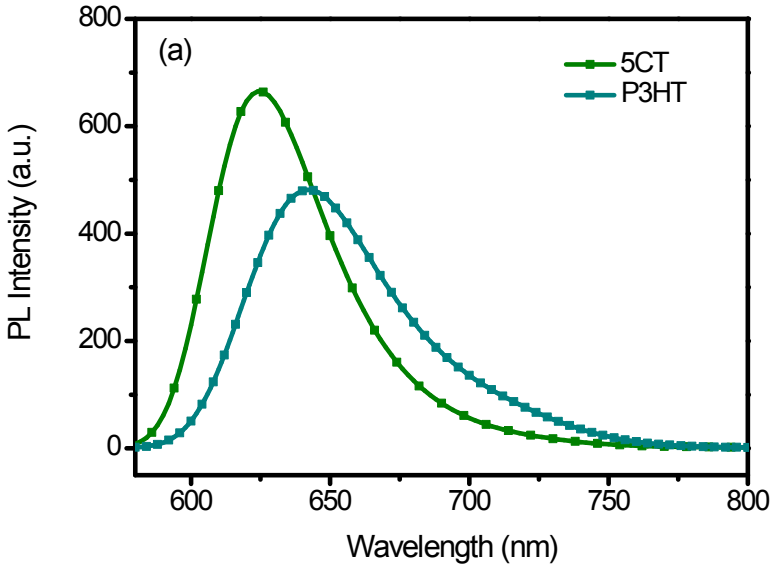
(a)
5CT
P3HT
PL Intensity (a.u.)
Wavelength (nm)
0
200
400
600
800
600
650
700
750
800

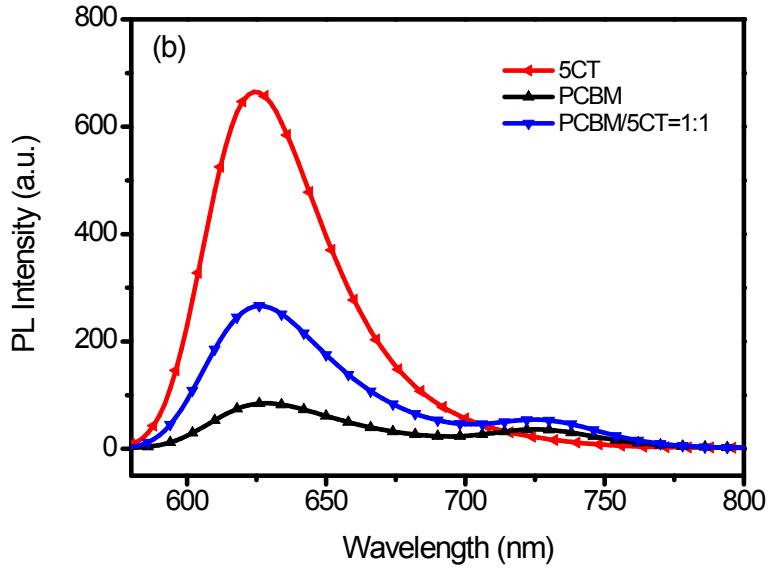
(b)
5CT
PCBM
PCBM/5CT=1:1
PL Intensity (a.u.)
Wavelength (nm)
0
200
400
600
800
600
650
700
750
800

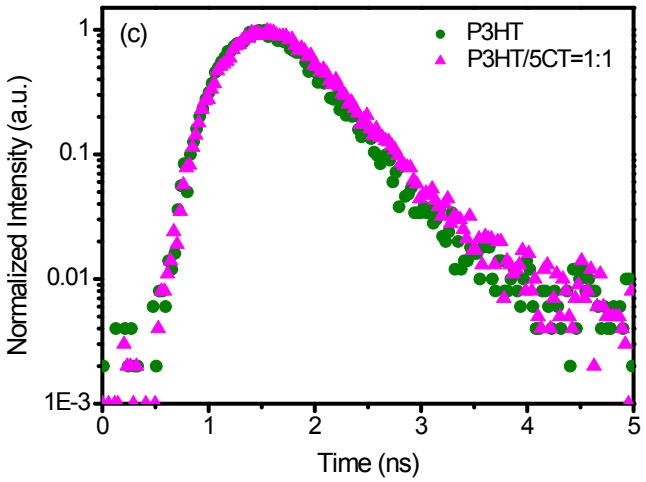

Figure S5. The photoluminescence spectra of (a) 5CT and P3HT, (b) PCBM/5CT blends and (c) photoluminescence lifetime decay of the P3HT and P3HT/5CT blend.

The photoluminescence properties were examined at the excitation wavelength of 480 nm on an LS-55 (Perkin-Elmer), for which the specimens were prepared by drop-casting. The concentration of the PCBM, P3HT, 5CT in chloroform was maintained at 10 mg/mL, and the PCBM/5CT (1:1 in weight ratio) and PCBM/P3HT (1:1 in weight ratio) blends in chloroform was 20 mg/mL. The static photoluminescence spectra are shown below. In **Figure S5a**, both of 5CT and P3HT exhibit a relatively strong emission peak. It is noted that the LUMO level of P3HT and 5CT is -3.20 eV and -3.36 eV. The LUMO level of the accepter should be at least 0.3 eV lower than that of the donor to drive charge separation after exciton formation. Thus, the exciton may not be able to dissociate at the P3HT and 5CT interface due to the relatively low energy level gap. In **Figure S5b**, it is observed that the intensity of emission peak at about 624 nm attributing to 5CT molecules is relatively strong. After the incorporation of PCBM molecules, the intensity of the emission peak sharply depressed, which should be corresponding to the energy transfer between 5CT and PCBM molecules. Furthermore, the emission peak at about 728 nm contributing to PCBM in PCBM/5CT blend slightly increased, indicating of the energy transfer from 5CT to PCBM.

To further explore the energy transfer between P3HT and 5CT, the time-resolved photoluminescence spectra of P3HT and P3HT/5CT=1:1 were recorded by Edinburgh Instrument FLS920 at an excitation wavelength of 650 nm. The PL lifetime was calculated by fitting data to a single exponential decay function.[4]

$$I=I_0e^{-t/\tau} \quad (4)$$

where I_0, τ and I are the initial PL intensity, the PL lifetime, and the PL decay intensity as a function of time (t), respectively. The PL lifetime profiles for the pristine P3HT and P3HT/5CT = 1:1 are given in **Figure S5c**, which, as expected, shows a PL lifetime of 580 ps for the pristine P3HT and a much similar PL lifetime of 599 ps for the P3HT/5CT. It declared that there has no charge-transfer interaction in the P3HT/5CT interface. However, the PL lifetime in the P3HT/PCBM/5CT blend could not be determined due to the limitation of the instrument.

In conclusion, the exciton generated by P3HT will not be able to dissociate at the interface of P3HT and 5CT junction. In contrast, the exciton generated by 5CT can dissociate at the PCBM/5CT interface.

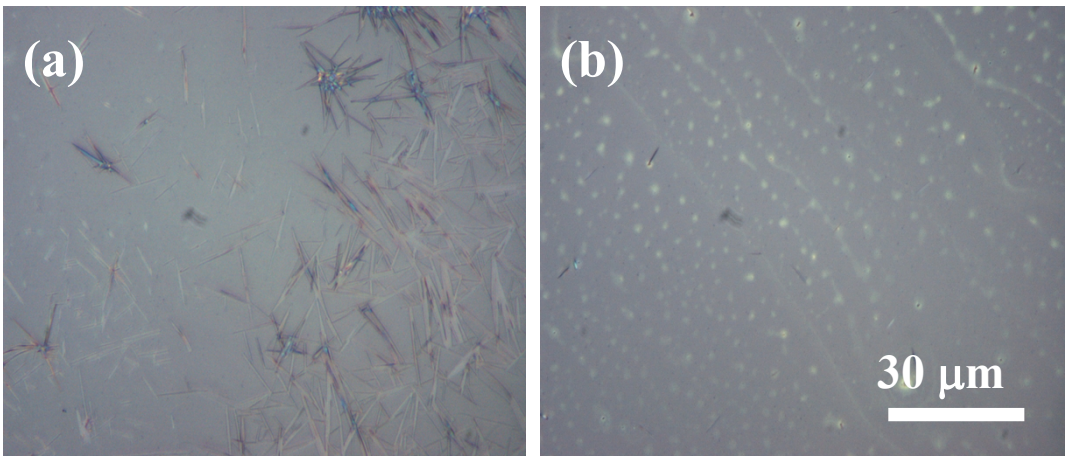

Figure S6. Dark-field POM images of 5CT films dropping on an ITO glass substrate via (a) the direct solvent evaporation method and (b) the electric field assisted treatment (300 V/mm) during the solvent evaporation process.

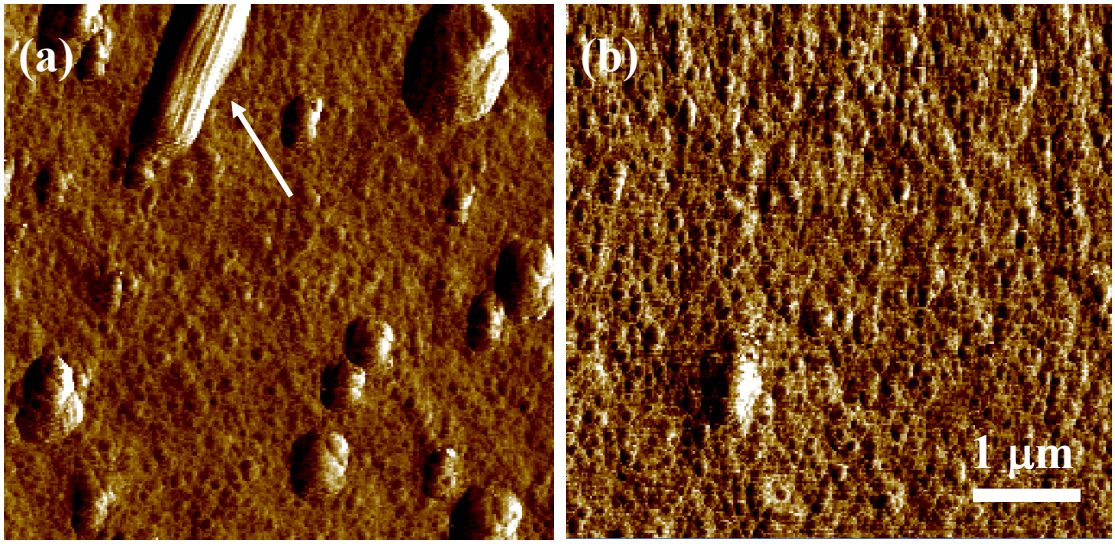

Figure S7. AFM images of P3HT/PCBM/5CT(1:1:0.06) films on the ITO substrate covered by a PEDOT:PSS layer at different conditions: (a) solvent slow drying and (b) in the presence of electric field of 600 V/mm. The aggregates contribute to the complexes composing of PCBM and 5CT.

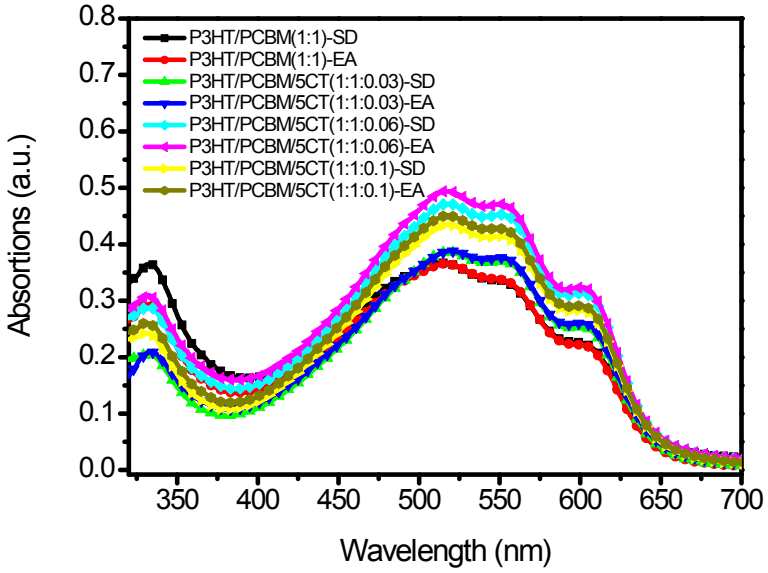

Figure S8. UV-vis spectra of the P3HT/PCBM/5CT blend films at different weight fraction of 5CT before and after electric field assisted treatment at 600 V/mm. The SD represents the slow drying while the EA refers to electric field assisted treatment.

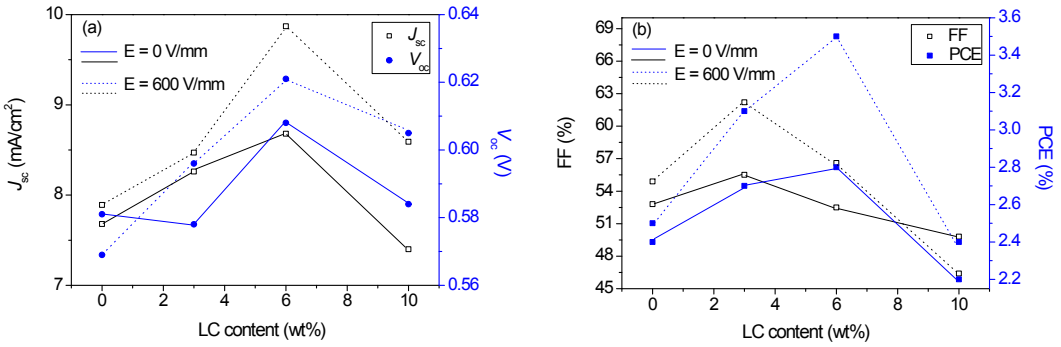

Figure S9. The relationship between the photovoltaic parameters of J_{sc}, V_{oc}, FF, PCE and 5CT content without electric field assisted treatment and after electric field assisted treatment at 600 V/mm.

References:

1. H. Q. Zhou, Y. Zhang, J. Seifter, S. D. Collins, C. Luo, G. C. Bazan, T. Q. Nguyen and A. J. Heeger, *Adv*. *Mater*., 2013, **25**, 1646-1652.
2. V. D. Mihailetchi, L. J. A. Koster, P. W. M. Blom, C. Melzer, B. Boer, J. K. J. Duren and R. A. J. Janssen, *Adv*. *Funct*. *Mater*., 2005, **15**, 795-801.
3. Y. Zhang and P. W. M. Blom, *Appl*. *Phys*. *Lett*., 2011, **98**, 143504.
4. Y. Kim and D. D. C. Bradley, *Curr*. *Appl*. *Phys*. 2005, **3**, 222-226.